DE GRUYTER Biomed. Eng.-Biomed. Tech. 2018; 63(5): 529–535

Tobias Heimpold, Frank Reifegerste*, Stefan Drechsel and Jens Lienig

# LED for hyperspectral imaging – a new selection method

https://doi.org/10.1515/bmt-2017-0120
Received July 19, 2017; accepted September 4, 2018; online first September 24, 2018

**Abstract:** Hyperspectral imaging (HSI) has become a sophisticated technique in modern applications such as food analyses, recycling technology, medicine, pharmacy and forensic science. It allows one to analyse both spatial and spectral information from an object. But hyperspectral cameras are still expensive due to their extended wavelength range. The development of new light-emitting diodes (LED) in the recent past enables another approach to HSI using a monochrome camera in combination with a LED-based illumination. However, such a system has a lower spectral resolution. Additionally, the growing supply of LED on the market complicates the selection of LED. In this paper, we propose a new time efficient selection method for the design process of an illumination. It chooses an optimised LED combination from an existing database to match a predefined spectral power distribution. Therefore, an algorithm is used to evaluate various LED combinations. Furthermore, the method considers the spectral behaviour of each LED in dependence of forward current and temperature of the solder point. Our method has already shown promise during the selection process for even spectral distributions which is demonstrated in the study. Additionally, we will show its potential for HSI illuminations.

**Keywords:** design process; illumination; light-emitting diodes; multiplexed; multispectral.

## Introduction

Hyperspectral imaging (HSI) recovers spatial and spectral data from an object of interest. Utilising not just the visible range but also the ultraviolet and infrared spectrum allows a more detailed analysis of the object's condition. Therefore, HSI has found its way into many modern applications such as medicine [1] and pharmacy [2], but also into food analyses [3], recycling technology [4] and forensic science [5].

In medical applications, HSI is mainly used for optical diagnostics on tissue and image-guided surgery [1]. HSI systems can be used to improve diagnostics by visualising tissue characteristics hidden for the human eye. This is shown in several publications and covers the area of cancer research [6–9], the detection of retina diseases [10–13], the observation of melanin and haemoglobin concentration in human skin [14, 15] and the detection of parasitic infestation [16]. Furthermore, first studies show, that a HSI system can also provide assistance during surgery [17, 18].

Different techniques to obtain a hyperspectral image have been developed in the past years using traditional optical filters or tuneable filters in front of a digital camera [19], multispectral filter arrays extending the three-channel Bayer pattern [20] or a multiplexed light-emitting diodes (LED) illumination with different types of LEDs in combination with a monochrome or traditional RGB camera [21].

Especially the last technique has shown much potential in recent years. The requirements on LED based illuminations are presented later in this paper.

LEDs offer several advantages such as low energy consumption, small size, cost effectiveness and fast switching capability in regard to conventional illuminations. Furthermore, the continued improvements of LED have led to a large supply of components over a wide spectral range in the recent years. It is now not only possible to build a multiplexed LED illumination, but to replace the traditional incandescent lamps with LED-based illuminations for cameras with tuneable filters or multispectral filter arrays. However, one disadvantage of LEDs is the dependency of their spectral behaviour from forward current and temperature of their solder point [22]. Thus, a LED illumination must stabilise both parameters during the imaging process to avoid drift in peak wavelength of the single LED spectra. So it is of high importance to choose the correct LED components for an efficient illumination.

The selection for a multiplexed LED illumination may seem rather simple: achieve a more or less uniform

***Corresponding author: Frank Reifegerste,** Institute of Electromechanical and Electronic Design, Faculty of Electrical and Computer Engineering, Dresden University of Technology, Helmholtzstr. 10, D-01069 Dresden, Germany, Phone: +49 351 463 36296, Fax: +49 351 463 37183, E-mail: Frank.Reifegerste@tu-dresden.de
**Tobias Heimpold, Stefan Drechsel and Jens Lienig:** Institute of Electromechanical and Electronic Design, Faculty of Electrical and Computer Engineering, Dresden University of Technology, Helmholtzstr. 10, D-01069 Dresden, Germany

distribution over the spectral range to obtain as much different spectral information as possible. However, the design of a replacement for an incandescent lamp or another special spectral power distribution is not that trivial. The possible combinations of LEDs and their different forward currents cannot be humanly surveyed in a reasonable design period. An algorithm is needed that selects an optimised combination of LED in regard to their characteristics to match a given spectral power distribution. The algorithm could also improve the selection process for multiplexed LED illuminations. The variation of the peak wavelength using different forward currents could reduce the number of needed LEDs to cover the same spectral range.

In this paper, we propose such a selection method based on an evolutionary algorithm to evaluate various LED combinations. Our method allows a time efficient selection of LED components from an existing database. The algorithm uses an accurate interpolation model to simulate the spectral behaviour of each LED in dependence of current and temperature. The resulting spectral behaviour of the illumination can be predicted with this model, as well. The algorithm uses this prediction in order to determine the suitability of a LED combination in regard to the predefined target distribution. The number of used colour channels can be set by the designer allowing him to find a trade-off between goodness-of-fit and the control effort for an additional LED channel.

The basic requirements for the algorithm are presented in the next section. Its methodology is explained in detail afterwards. The algorithm is used to select LEDs for three exemplary target distributions. A discussion of the results and the algorithm's actual limitations follows. Finally, we give a prospect of possible improvements on the algorithm's methodology to increase the quality of the found solutions and to decrease its runtime.

## Requirements

Figure 1 illustrates a multispectral imaging system with LED-based illumination. The computer needed to control both camera and illumination and to evaluate the captured hyperspectral image is not shown. The illustrations show the illumination part in detail.

It can be divided into a control part, the different colour channels including the LEDs, an optic to mix the light of the single LEDs and a light output to illuminate the object. Each LED channel can be operated individually. This allows either a multiplexed illumination where

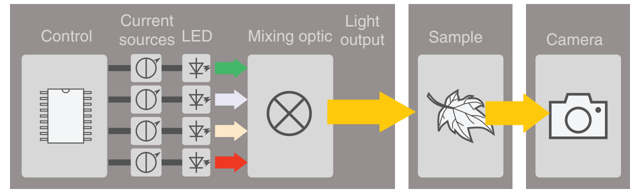


**Figure 1:** Hyperspectral imaging system with LED illumination.

the LEDs are switched on and off in sequence to capture a hyperspectral image with a monochrome camera or the LEDs can be operated in combination with different currents to simulate special spectral power distributions.

There are two different requirements for a LED-based illumination depending on the medical application. If the illumination is needed to extract the spectral information from infected and non-infected tissue, than it will have to cover a broad spectrum with an equally distributed power distribution. In most cases, this requires a spectrum form 400 to 1000 nm [1–21]. If the wavelength to distinguish between infected and non-infected tissue is already known, the illumination can concentrate on this wavelength area utilising the full potential of LEDs.

In this paper, we concentrate on the selection of the different LEDs to match one predefined spectral power distribution.

Our selection method needs three basic requirements to be defined by the designer in regard to the illumination's application:

- the target spectral power distribution $t(\lambda)$,
- the number of colour channels $n$ and
- a database with LEDs and LED models to choose from.

We chose to demonstrate our selection method with three exemplary spectral power distributions shown in Figure 2. They illustrate that the shape of the target distribution is not restricted as long as it does not contain negative intensities.

The goal for the selection process is to choose the combination of $n$ LEDs from a database which matches the target distributions best. As mentioned in the introduction, the designer will have to decide whether an additional colour channel is worth the effort. Later in this paper we will use four, six and eight colour channels to show the potential of our proposed method.

The database is a more complex matter. We have sampled various LEDs from the market for the past years. Their spectral behaviour in dependence of forward current and temperature of the solder point has been characterised in our experimental setup. Both parameters have been controlled and stabilised during the measurement.

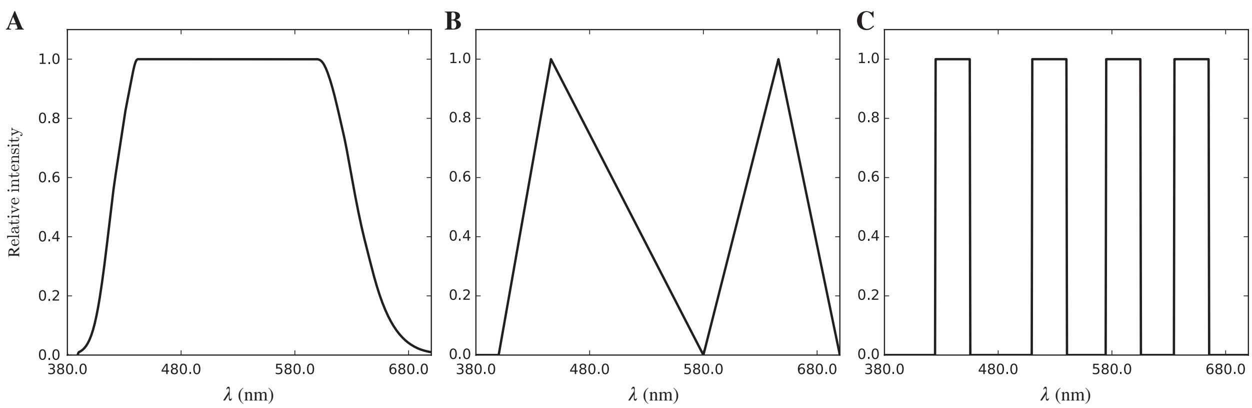


**Figure 2:** Different target distributions to demonstrate the algorithms potential.
(A) Equal energy spectrum within the visual range, faded out at the borders, (B) synthetic triangular spectrum, (C) synthetic narrow band spectrum.

The spectral information obtained by the characterisation is used for an interpolation model. It uses cubic splines and Coons' patches [23, 24] to interpolate the spectral behaviour. This model allows an accurate prediction of the spectral power distributions of a LED or a combination of several LEDs within the measurement limits. There are now more than 200 different LEDs in our database for the selection method to choose from.

## The selection method

With the target distribution $t(\lambda)$ defined and the LED characteristics stored in a database, we use a metaheuristic approach to select the LEDs for the illumination. The methodology of the heuristic is shown in Figure 3. It is based on an evolutionary algorithm described in [25]. A set of solutions is created as parent generation. Each solution represents a combination of $n$ different LEDs randomly chosen from the database. However, the first tests showed that the number of possible combinations is too high to be searched in a reasonable design period. Furthermore, the designer cannot use his knowledge to improve the search behaviour. For example, the distribution in Figure 2B could be matched by using one blue and one red LED in two different channels. This knowledge of the designer can be used to limit the search area and to avoid undesired solutions with, for example, only blue LEDs.

A constraint for each channel can model this knowledge: colour groups. The LEDs in the database have been categorised into seven colour groups: blue (bl), green (gn), amber (am) red (rd), warm-white (ww), neutral-white (nw) and cool-white (cw). A further expansion of these groups is easily possible to cover the ultraviolet and

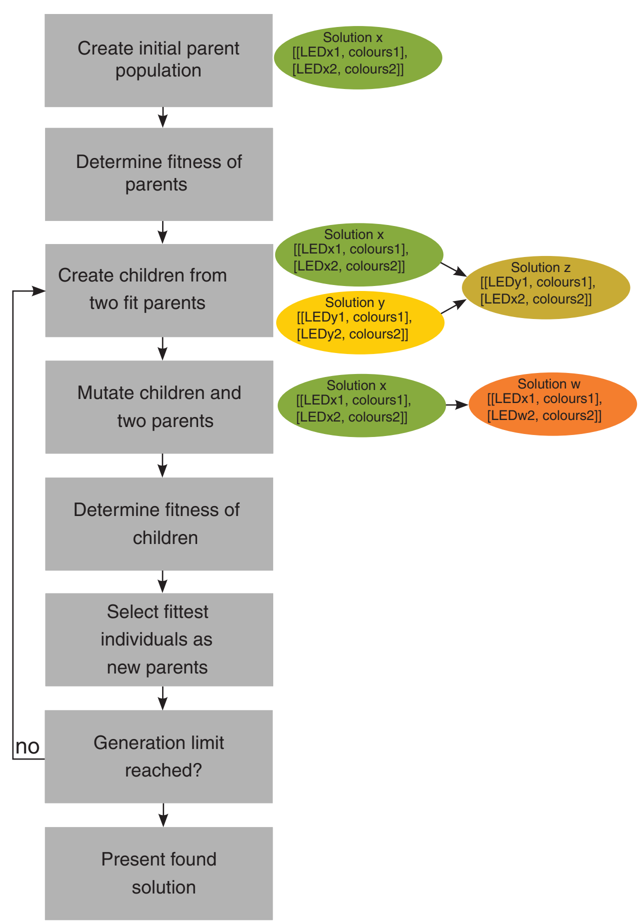


**Figure 3:** Methodology of the proposed selection method with a two channel illumination example.

infrared range of the spectrum. The designer can use these colour groups to limit the search area for each channel individually. One can explicitly force the algorithm to use, for example, only blue LEDs in one channel and red or amber LEDs in another one. Each channel can have more than one colour group. The algorithm ensures that no LED is used twice in a combination.

We now have a set of combinations of different LEDs as the current parent generation. Each solution contains the information about the $n$ colour channels: the actual selected LED from the database and the colour groups for the algorithm to choose a new LED from for each colour channel. These $n$ data tuples represent the genetic information used in evolutionary algorithms to search for new solutions.

The next step of the algorithm is to evaluate the fitness of the current parent generation using the method of least square errors. It is explained in detail after this section.

An evolutionary algorithm has two basic operations to improve the fitness of a solution: crossover and mutation. The crossover operation uses parents from the current generation and their genetic information to create a new solution (an offspring/a child). In our algorithm, an offspring is created by using two parents with high fitness. The algorithm constructs an offspring with $n$ colour channels. The data tuple for each channel is chosen randomly from either the two parents. The crossover operation ensures that the new solution differs at least in one colour channel in regard to its parents. The mutation operation changes a part of the genetic information in a parent to create a new solution. It can also be used on an offspring. In our algorithm, the mutation operation chooses a new LED from the database for one colour channel of the LED combination. The predefined colour groups of the channel are respected by the mutation operator. It also ensures that no LED is used twice in a combination. Our algorithm uses the mutation operation on both groups: parents and children to increase the genetic diversity of the population. So, more different LED combinations are searched.

The fitness of the children is determined next. Afterwards, the fittest individuals are used to form the next parent generation. This procedure is repeated for some generations.

## The fitness function

The target distribution has to be matched by using different forward currents $I_i$ at solder point temperatures $T_i$ for each LED. The combined distribution $s(\lambda)$ of a LED mix spectrum can be written as sum of the single LED distributions $s_i(\lambda, I_i, T_i)$:

$$s(\lambda) = \sum_{i=1}^{n} s_i(\lambda,\ I_i,\ T_i) \tag{1}$$

A variation of the solder point temperature has proven to be impractical because of the extended effort to control each LED channel individually. The solder point temperature is defined as equal and constant for all LED with $T_c$. The designer should choose a temperature $T_c$ which can be reached in the target application with an appropriate thermal design.

The method of least square error can be used to determine the forward currents where the target distribution $t(\lambda)$ is matched best using the modelled LED characteristics from the database:

$$E = \int \left( t(\lambda) - \sum_{i=1}^{n} s_i(\lambda,\ I_i,\ T_c) \right)^2 \mathrm{d}\lambda \rightarrow \min \tag{2}$$

The sum of the errors $E$ is used to determine the goodness of the solution.

However, the model uses cubic splines to interpolate the nonlinear spectral behaviour in dependence of forward current and temperature. Because of this nonlinear model the minimisation problem cannot be solved analytically [24].

In order to calculate the problem nevertheless, the following approach has proven to work. We use the spectral correction method proposed by Henker et al. to simplify the problem [26, 27]. Therefore, we write the combined distribution as a linear combination of the LED spectra using the forward current $I_j$ for each channel:

$$s(\lambda) = \sum_{i=1}^{n} c_i \cdot s_i(\lambda, I_j, T_c) \tag{3}$$

For reasons of computation time the same forward current $I_j$ (please note index $j$) is assumed for all LED. This is permissible because solutions with very different operating currents are unfavourable. With (2) and (3) follows:

$$E = \int \left( t(\lambda) - \sum_{i=1}^{n} c_i \cdot s_i(\lambda, I_j, T_c) \right)^2 \mathrm{d}\lambda \rightarrow \min \tag{4}$$

With $I_j$ and $T_c$ being constant, the spectral distribution of the LEDs $s_i(\lambda,\ I_j,\ T_c)$ is now given by the interpolation model and does not contain an unknown variable anymore. Eq. (4) can now be solved with an analytic approach to derive the unknown factors $c_i$ [26, 27].

The factors $c_i$ can be interpreted as the number of LED needed for each colour channel to match the target distribution with a given current $I_j$. However, we want to know the current for each channel where the target distribution is matched with one LED in each channel. Thus, Eq. (4) is solved for a number of different forward currents $I_j$.

This results in a dependency of the factor $c_i$ from these different currents $I_j$. This dependency can be interpolated by a cubic spline as a function with the calculated supporting points $c_i(I_j)$. Its parameters are fitted with the least square method. As last step, the current $I_c$ can be determined where $c_i(I_j)$ is equal to one:

$$c_i(I_c) = 1 \tag{5}$$

The current $I_c$ is approximately the current where the target distribution is matched with one LED and the sum of least square errors of Eq. (2) is near its minimum. Despite the simplification of equal forward currents $I_j$ the approach has proven to be more time efficient than a numeric solution for Eq. (2) with an acceptable error.

Finally, the goodness-of-fit of the LED combination is calculated with:

$$E = \int \left( t(\lambda) - \sum_{i=1}^{n} s_i(\lambda, I_c, T_c) \right)^2 \mathrm{d}\lambda \tag{6}$$

## Results

We used our selection method to match the target distributions in Figure 2 with LEDs from our database. The results for four, six and eight colour channels are shown in Figure 4. We used 18 parents, nine children and nine mutated parents each generation. The algorithm ran five generations. This adds up to 180 different combinations searched by the algorithm. Table 1 lists the identifiers for the found LEDs for two different runs of the selection method for the target distribution Figure 4B with four, six and eight channels. The combinations shown in Figure 4 are set in bold letters. The colour groups used to limit the search area are shown in parenthesis below the identifiers. The colour group of the chosen LED is underscored. Table 2 lists the fitness of two runs of the algorithm for each target distribution shown in Figure 2. The fitness of the solutions shown in Figure 4 is set in bold letters.

## Discussion and limitations

The results show that the algorithm is able to choose LEDs from the database to match the given target distribution. It needs approximately 25 s per channel with the used number of individuals and generations using a state-of-the-art desktop PC with an Intel® Core™ i7-6700 @ 3.4 GHz. The LED models and the selection method are implemented in Python 2.7. However, further tests are needed to determine whether the runtime scales linear to the number of colour channels.

The results are promising for even distributions like Figure 4A and B. The results show that a higher number of colour channels improve the goodness-of-fit as one expects.

One drawback of the algorithm is its non-deterministic behaviour. Each run with the same constraints and settings can result in a different combination as final solution. This illustrates the identifiers in Table 1. This behaviour cannot be changed due to the evolutionary approach used for the selection method which chooses LEDs randomly at some point. To improve the search behaviour, more constraints could be introduced, for example, limiting the manufacturers of the LEDs to choose from or the packages of the LED.

The algorithm's potential for the design of multiplexed LED illuminations is also limited at the moment. The target distribution in Figure 2C was designed to represent such

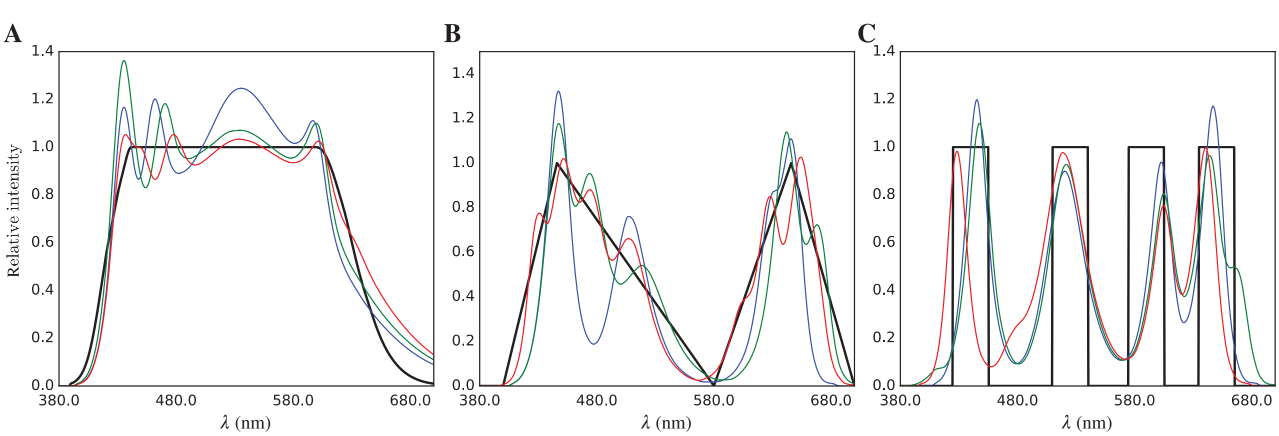


**Figure 4:** Best LED combination found with the selection method with four (blue), six (green) and eight (red) colour channels.

**Table 1:** Selected LEDs for target distribution shown in Figure 2 (B) for four, six and eight colour channels; the number represents the LED-index in the database.

| Test run | LED1 | LED2 | LED3 | LED4 | LED5 | LED6 | LED7 | LED8 |
|---|---|---|---|---|---|---|---|---|
| B-4-1 | **18** (bl) | **117** (gn) | **232** (am) | **119** (rd) | – | – | – | – |
| B-4-2 | 83 (bl) | 117 (gn) | 115 (am) | 86 (rd) | – | – | – | – |
| B-6-1 | **18** (bl) | **102** (bl, gn) | **6** (gn) | **4** (am) | **3** (rd, am) | **95** (rd) | – | – |
| B-6-2 | 83 (bl) | 17 (bl, gn) | 116 (gn) | 232 (am) | 73 (rd, am) | 95 (rd) | – | – |
| B-8-1 | **113** (bl, gn) | **75** (bl, gn) | **117** (bl, gn) | **55** (bl, gn) | **45** (rd, am) | **49** (rd, am) | **70** (rd, am) | **73** (rd, am) |
| B-8-2 | 17 (bl, gn) | 83 (bl, gn) | 80 (bl, gn) | 47 (bl, gn) | 15 (rd, am) | 107 (rd, am) | 111 (rd, am) | 104 (rd, am) |

Solutions shown in Figure 4 are set in bold letters; the colour group of the chosen LED is underscored.

**Table 2:** Best solution found with the selection method in two independent runs for the target distributions shown in Figure 2; the number represents the measure of the goodness of fit.

| Test run 1 | Fitness | Test run 2 | Fitness |
|---|---|---|---|
| **A-4-1** | **9.7** | A-4-2 | 11.4 |
| **A-6-1** | **11.4** | A-6-2 | 16.2 |
| **A-8-1** | **6.4** | A-8-2 | 9.0 |
| **B-4-1** | **40.4** | B-4-2 | 40.5 |
| **B-6-1** | **14.6** | B-6-2 | 15.5 |
| **B-8-1** | **7.4** | B-8-2 | 10.5 |
| **C-4-1** | **73.7** | C-4-2 | 121.6 |
| **C-6-1** | **86.8** | C-6-2 | 89.4 |
| **C-8-1** | **119.5** | C-8-2 | 126.6 |

Solutions shown in Figure 4 are set in bold letters.

an illumination. However, the algorithm's fitness function expects a simultaneous operation of the LED channels. This is shown by the results for the target distribution in Figure 4C. Especially the intensities in the wavelength ranges between the rectangles are too high and decrease the goodness-of-fit, because the algorithm cannot handle the multiplexed operation of the LED channels yet. This problem gets even worse with a higher number of LED channels, as shown by Table 2. The improvement of the algorithm to design multiplexed LED illuminations is part of actual research in our group.

## Summary

We proposed a new selection method for LED components during the design process of special spectral power distributions. The algorithm is based on an evolutionary approach and considers the spectral behaviour of each LED. The designer can use his knowledge to improve the search behaviour by defining certain constraints. First experimental results showed the potential of the new selection method for even target distributions. The improvement of the algorithm's search behaviour by modelling the knowledge of the designer as constraints is part of future work.

**Author Statement**
**Research funding:** Authors state no funding involved.
**Conflict of interest:** Authors state no conflict of interest.
**Informed consent:** Informed consent is not applicable.
**Ethical approval:** The conducted research is not related to either human or animals use.

## References

[1] Lu G, Fei B. Medical hyperspectral imaging: a review. J Biomed Opt 2014;19:010901.
[2] Gendrin C, Roggo Y, Collet C. Content uniformity of pharmaceutical solid dosage forms by near infrared hyperspectral imaging: a feasibility study. Talanta 2007;73:733–41.
[3] Gowen A, O'Donnell C, Cullen P, Downey G, Frias J. Hyperspectral imaging – an emerging process analytical tool for food quality and safety control. Trends Food Sci Technol 2007;18:590–8.
[4] Serranti S, Gargiulo A, Bonifazi G. Characterization of post-consumer polyolefin wastes by hyperspectral imaging for quality control in recycling processes. Waste Manage 2011;31:2217–27.
[5] Edelman G, Gaston E, van Leeuwen T, Cullen P, Aalders M. Hyperspectral imaging for non-contact analysis of forensic traces. Forensic Sci Int 2012;223:28–39.
[6] Akbari H, Halig LV, Schuster DM, Osunkoya A, Master V, Nieh PT, et al. Hyperspectral imaging and quantitative analysis for prostate cancer detection. J Biomed Opt 2012;17:076005-1-10.
[7] Akbari H, Uto K, Kosugi Y, Kojima K, Tanaka N. Cancer detection using infrared hyperspectral imaging. Cancer Sci 2011;102:852–7.
[8] Pratavieira S, Andrade C, Salvio A, Bagnato V, Kurachi C. Optical imaging as auxiliary tool in skin cancer diagnosis. In: Skin Cancers – Risk Factors, Prevention and Therapy. Rijeka, Croatia: InTech; 2011:159–72.
[9] Vo-Dinh T. A hyperspectral imaging system for in vivo optical diagnostics. IEEE Eng Med Biol 2004;23:40–9.
[10] Schweizer J, Hollmach J, Steiner G, Knels L, Funk RH, Koch E. Hyperspectral imaging – a new modality for eye diagnostics. Biomed Eng Biomed Tech 2012;57:293–6.
[11] Brydegaard M, Guan Z, Svanberg S. Broad-band multispectral microscope for imaging transmission spectroscopy employing an array of light-emitting diodes. Am J Phys 2009;77:104–10.

[12] Harvey AR, Lawlor J, McNaught AI, Williams JW, Fletcher-Holmes DW. Hyperspectral imaging for the detection of retinal disease. Proc SPIE 2002;4816:325–35.
[13] Everdell N, Styles I, Claridge E, Hebden J, Calcagni A. Multispectral imaging of the ocular fundus using LED illumination. Rev Sci Instrum 2010;81:093706.
[14] Koprowski R, Wilczy'nski S, Wróbel Z, Kasperczyk S, Błońska-Fajfrowska B. Automatic method for the dermatological diagnosis of selected hand skin features in hyperspectral imaging. Biomed Eng Online 2014;13:47.
[15] Klaessens J, De Roode R, Verdaasdonk RM, Noordmans HJ. Hyperspectral imaging system for imaging O2Hb and HHb concentration changes in tissue for various clinical applications. Proc SPIE 2011;7890:78900R–10R.
[16] Zoueu JT, Ouattara S, Toure A, Safi S, Zan ST. Spectroscopic approach of multispectral imaging of plasmodium falciparum-infected human erythrocytes. 2009 3rd ICTON Mediterranean Winter Conference (ICTON-MW), Angers, France; 2009:1–7.
[17] Sobottka SB, Meyer T, Kirsch M, Koch E, Steinmeier R, Morgenstern U, et al. Intraoperative optical imaging of intrinsic signals: a reliable method for visualizing stimulated functional brain areas during surgery. J Neurosurg 2013;119:853–63.
[18] Panasyuk SV, Yang S, Faller DV, Ngo D, Lew RA, Freeman JE, et al. Medical hyperspectral imaging to facilitate residual tumor identification during surgery. Cancer Biol Ther 2007;6:439–46.
[19] Schmitt F. Multispectral color image capture using a liquid crystal tunable filter. Opt Eng 2002;41:25–32.
[20] Shrestha R, Hardeberg JY, Khan R. Spatial arrangement of color filter array for multispectral image acquisition. In: Widenhorn R, Nguyen V, editors. Sensors, Cameras, and Systems for Industrial, Scientific, and Consumer Applications XII. San Francisco Airport, CA, USA: SPIE; 2011.
[21] Park JI, Lee MH, Grossberg MD, Nayar SK. Multispectral imaging using multiplexed illumination. IEEE 11th International Conference on Computer Vision, Rio de Janeiro, Brazil; 2007:1–8.
[22] Reifegerste F, Lienig J. Modelling of the temperature and current dependence of LED spectra. J Light Visual Environ 2008;32:288–94.
[23] Barnhill R. Coons' patches. Comput Ind 1982;3:37–43.
[24] Schwarz HR, Köckler N. Numerische Mathematik. 8th ed. Wiesbaden: Vieweg&Teubner; 2009.
[25] Weicker K. Evolutionäre Algorithmen/Lehrbuch. 3rd ed. Wiesbaden: Springer Vieweg; 2015.
[26] Henker S, Schlüssler J-U, Schüffny R. Concept of Color Correction on Multi-Channel CMOS Sensors. Sydney, Australia: DICTA; 2003:771–80.
[27] Henker S, Schlüssler J-U, Schüffny R. White Balancing with Multi-Channel CMOS Sensors. Proceedings Image and Vision Computing, New Zealand; 2005.